7.2A OROGRAPHIC ENHANCEMENT OF PRECIPITATION IN MIDLATITUDES: RESULTS FROM MAP AND IMPROVE II

Socorro Medina* and R. A. Houze, Jr.
University of Washington, Seattle

1. INTRODUCTION

When midlatitude baroclinic systems move over a mountain range, the precipitation from the system intensifies over and sometimes upwind of the slope of the mountain barrier. The maximum precipitation occurs on the lower windward slopes in almost immediate response to the orographically induced lifting of the air such that the maximum precipitation may occur well below the summit of the range (e.g., Frei and Schaer 1998). How this rapid response to the orographic lifting occurs is the central question of orographic enhancement of midlatitude baroclinic precipitation. Smith (1979) called attention to this question by expressing the rapid fallout of the condensate produced by the orographic component of the lifting in terms of an efficiency. This efficiency may be thought of as the ratio of rainfall on the mountainside to the amount of water condensed in the upslope flow. Reviewing the literature, he noted that this ratio was typically high: "…It is…surprising in light of the difficulties in forming precipitation-size particles, to find release efficiencies of 70% to 100%, …" That is, this high efficiency could only occur if there was a rapid conversion of the condensate generated by the orographic uplift to particles large enough to fall out quickly before being advected over the crest of the mountain range. He asked further, how "is it possible to convert such a high fraction of the condensed water into precipitation?" Since microphysical processes control the growth rate of precipitation particles, the answer to this question is a matter of determining how the microphysical processes accelerate the growth of precipitation particles in the upslope flow. Current research on orographic enhancement of precipitation focuses on answering the question of how microphysical processes are invigorated to account for the efficiency of the orographic precipitation enhancement. This paper reviews some recent progress toward this end.

2. MICROPHYSICS PROMOTED BY CELLULAR OVERTURNING

The microphysical processes available that quickly convert condensate to precipitation-sized particles are the ones of accretion: coalescence, riming, and aggregation. The efficiency of the orographic enhancement of the precipitation requires dynamical mechanisms that favor accretion processes over the lower windward slopes. Below the 0ºC level, growth by coalescence (cloud droplets quickly combining to form raindrops and pre-existing raindrops scavenging out the new cloud drops) can cause the condensate produced by the orographic lifting to fall quickly to the ground. Above the 0ºC level, aggregation (ice particles combining with each other) may produce particles big enough to fall into the melting layer and thence downward as raindrops. Also above the 0ºC level, ice particles growing by riming (accreting supercooled droplets) may quickly scavenge the cloud droplets newly condensed in the orographic uplift. The riming will make the snow particles formed by aggregation heavier so they fall out more quickly; this process can produce even more rapidly falling graupel particles if the amount of riming is sufficient.

If air rises smoothly over a mountain range, and the hydrometeors do not grow sufficiently by accretion, the condensed particles may be carried over the mountain range rather than fall out on the windward side (Hobbs et al. 1973). The question becomes, what dynamical processes promote the vigorous growth of particles by accretion, so that they become large enough to fall out quickly on or ahead of the lower windward slopes of a mountain range? Smith (1979, see his Fig. 26) suggested that cellular overturning superimposed on the upslope flow could promote the efficiency of the fallout of the precipitation particles growing in the upslope flow. The idea is that the small-scale updrafts, if occurring at an appropriate altitude, could generate liquid water contents high enough to accelerate both the growth of liquid drops by coalescence at low levels and by riming above the 0ºC level. The generally turbulent air motions would also promote the collision and aggregation of ice particles. The downward branches of overturning cells re-evaporate moisture in the upslope flow at the same time that the upward motions enhance precipitation growth. The precipitation particles whose growth has been enhanced in the updrafts avoid this re-evaporation by falling quickly out of the overturning layer.

3. CELLULAR OVERTURNING AS SEEN IN RECENT FIELD CAMPAIGNS

How does cellular overturning arise within this upslope flow? It is often assumed that a layer of

* *Corresponding author address:* Socorro Medina, Univ. of Washington, Dept. of Atmospheric Sciences, Seattle, WA 98195; e-mail: socorro@atmos.washington.edu.

potentially unstable air becomes saturated as the upslope flow ascends the terrain and that buoyant convection results in that layer. Several cases of baroclinic systems observed over the European Alps in the Mesoscale Alpine Program (MAP) exhibited an apparent release of potential instability over the first steep rise of the terrain. Medina and Houze (2003a) showed that this was occurring in MAP IOP2b. We have found similar behavior in IOP3 and IOP5 (Medina and Houze 2003b). Polarimetric radar data show evidence of graupel forming in the cells over the first main peak of the terrain. Yuter and Houze (2003) examined vertically pointing S-band radar data for IOP2b to show that the observed cellular updrafts were consistent with precipitation growth by coalescence at low levels and riming above the 0ºC level. These cases showed large precipitation accumulations on the lower slopes of the Alps.

In other MAP cases, IOP8 and IOP14, the upstream flow was potentially stable and the lowest level flow was blocked. However, above about 1 km, the flow was upslope and a large enhancement of precipitation again occurred on the lower slopes of the Alps. We have also examined a case in the Improvement of Microphysical PaRameterization through Observational Verification Experiment II (IMPROVE II, Stoelinga et al. 2003). This storm was moving over the Cascade Mountains of Oregon from the Pacific. The upstream flow was potentially stable in this case as well. In all three of these potentially stable cases, the precipitation exhibited a highly layered structure with a well-defined bright band at the melting layer. Despite this generally stratiform character, high resolution vertically pointing S-band radar data in all three cases showed cellular structure in the bright band and fallstreaks emanating from these cells (see IOP8 example in Yuter and Houze 2003). In all three cases, there was a strong wind shear in the lower troposphere. The case observed in IMPROVE II illustrates the characteristics of these stable cases. A vertical cross section across the Cascade Range shows the mean structure observed by the NCAR S-Pol radar for a 3-hr period of the storm (Fig. 1). The radar reflectivity (dBZ) shows a pronounced bright band extending over the windward slope of the range (Fig. 1a). The mean radial velocity data for the same time period show upslope flow with a strong shear between 1 and 3 km (Fig. 1b). The polarimetric particle identification algorithm (a version of the method of Vivekanandan et al. 1999) shows dry snow aloft and wet snow below, with a narrow layer sandwiched in between that is characterized by low differential reflectivity (ZDR) combined with high reflectivity (Fig. 1c). This layer lies in the upper portion of the melting layer and is consistent with the presence of dry aggregate snowflakes. Aircraft samples of ice particles in this layer indicate that the particles were aggregates with evidence of riming (Fig. 2). Thus, the aircraft data are consistent with the radar polarimetry.

Since the upstream flow was potentially stable in the IMPROVE II case, the aggregation and riming active just above the melting level cannot be explained by buoyant convection resulting from release of potential instability. However, strong mechanical turbulence was possible. The strong flow of stable air over the rough underlying terrain would have supported gravity waves. In addition, the strong shear in the 1-3 km layer would have engendered shear-driven turbulence. The Richardson Number in the shear layer was ~0.25. We suggest that the turbulence in the flow over the windward slopes was sufficient to facilitate aggregation and riming in the upward branches of overturning cells in this mechanical turbulence. Wind profiler data obtained in IMPROVE II support this hypothesis. Figure 3 is a time series of data from a NOAA/ETL wind profiler and vertically pointing S-band radar at McKenzie Bridge, Oregon, on the windward slope and from the S-Pol radar looking east over the windward slopes. The profiler shows maximum wind shear between 2000 UTC 13 December and 0400 UTC 14 December 2001 (Fig. 3a). The vertically pointing S-band radar showed fine-scale cells of upward radial velocity (particle velocity, uncorrected for fallspeed) during the period of strong shear (Fig. 3b). The negative (upward) radial velocities in the 2-3 km layer frequently reached values of several meters per second during this period (Fig. 3c). The strong turbulent motions would have promoted aggregation, and the magnitude of the peak vertical velocities was sufficient to promote the growth of the aggregates by riming, possibly even forming some graupel. The S-Pol polarimetric radar data during this period showed the most frequent joint occurrence of high dBZ and low ZDR (Fig. 3d).

The updraft cells seen in Fig. 3b appear to be cut off at a height of 1.5-2 km. The cells probably extended to lower levels. However, because they extended below the melting layer, downward velocities of raindrops overwhelmed the upward air motions. If the updrafts extended to lower levels, they would have further enhanced precipitation fallout by promoting coalescence ("warm rain") growth at low levels, as has been noted by Neiman et al. (2002) over the northern California coastal range.

It is possible that cooling of the air by melting may cause some convective overturning in the melting layer, and this process could enhance other turbulent motions. However, the convective overturning layer seen in Fig. 3b seems too vertically extensive to be the result solely of cooling confined to the melting layer, and it thus appears that mechanical turbulence may be an effective producer of the overturning required to excite the accretional growth processes even in the absence of buoyancy instability.

4. CONCLUSIONS

Thus, recent results from MAP and IMPROVE II indicate that strong, sheared flow over the rough terrain of the windward slope of a major mountain range has the ability to enhance baroclinic precipitation via cellular motions (as suggested by Smith 1979) even if the flow is potentially stable and buoyant motions are absent. It thus appears that any strong moist flow over the windward slope of a rugged mountain range has the ability to excite accretional growth processes (coalescence, aggregation, and riming) on the microphysical scale by cellular overturning of the upslope flow, even in the absence of potential instability. This tendency for strong upslope flow in baroclinic storms passing over mountain ranges nearly always to have a layer of air that will overturn (mechanically or buoyantly) may explain why the orographic enhancement is so “efficient.”

ACKNOWLEDGMENTS: This work was supported by National Science Foundation Grant ATM-0221843.

5. REFERENCES

Frei, C., and C. Schaer, 1998: A precipitation climatology of the Alps from high-resolution rain gauge observations. *Int. J. Climatol.*, **18**, 873-900.

Hobbs, P. V., R. C. Easter, and A. B. Fraser, 1973: A theoretical study of the flow of air and fallout of solid precipitation over mountainous terrain. Part II: Microphysics. *J. Atmos. Sci.*, **30**, 813-823.

Medina, S., and R. A. Houze, Jr., 2003a: Air motions and precipitation growth in alpine storms. *Quart. J. Roy. Meteor. Soc.*, special MAP issue, **129**, 345-371.

Medina, S., and R. A. Houze, Jr., 2003b: Orographic precipitation in potentially unstable Alpine storms. Preprints, ICAM/MAP Meeting, Brig, Switzerland, 19-23 May.

Neiman, P. J., and co-authors, 2002: The statistical relationship between upslope flow and rainfall in California's coastal mountains: observations during CALJET. *Mon. Wea. Rev.*, **130**, 1468-1492.

Smith, R. B., 1979: The influence of mountains on the atmosphere. *Adv. Geophysics*, **21**, 87-230.

Stoelinga, M. T., P. V. Hobbs, C. F. Mass, J. D. Locatelli, B. A. Colle, R. A. Houze, Jr., A. L. Rangno, N. Bond, B. F. Smull, R. Rasmussen, G. Thompson, and B. Colman, 2003: Improvement of Microphysical Parameterizations through Observational Verification Experiments (IMPROVE). *Bull. Amer. Meteor. Soc.*, conditionally accepted.

Vivekanandan, J., and co-authors, 1999: Cloud microphysics retrieval using S-band dual-polarization radar measurements. *Bull. Amer. Meteor. Soc.,* **80**, 381-388.

Yuter, S. E., and R. A. Houze, Jr., 2003: Microphysical modes of precipitation growth determined by S-band vertically pointing radar in orographic precipitation during MAP. *Quart. J. Roy. Meteor. Soc.*, special MAP issue, **129**, 455-476.

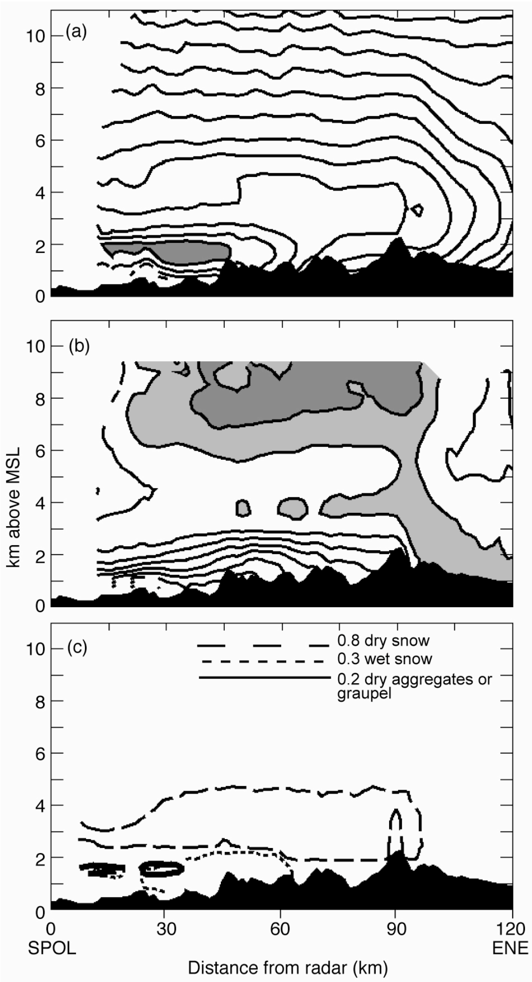

Figure 1. Vertical cross section of NCAR S-pol radar data extending from the radar site, located on the lower left corner of the panels, across the Cascade Range to the east-northeast. Topography is shown in the lower part of each panel. The fields in the panels have been either accumulated or averaged over 2100 UTC 13 December - 0000 UTC 14 December 2001. (a) Mean reflectivity contoured every 5 dBZ, values >36 shaded. (b) Mean radial velocity contoured every 3 m/s, values >39.5 m/s dark-shaded, values >36.5 light-shaded. (c) Frequency of occurrence of particle types.

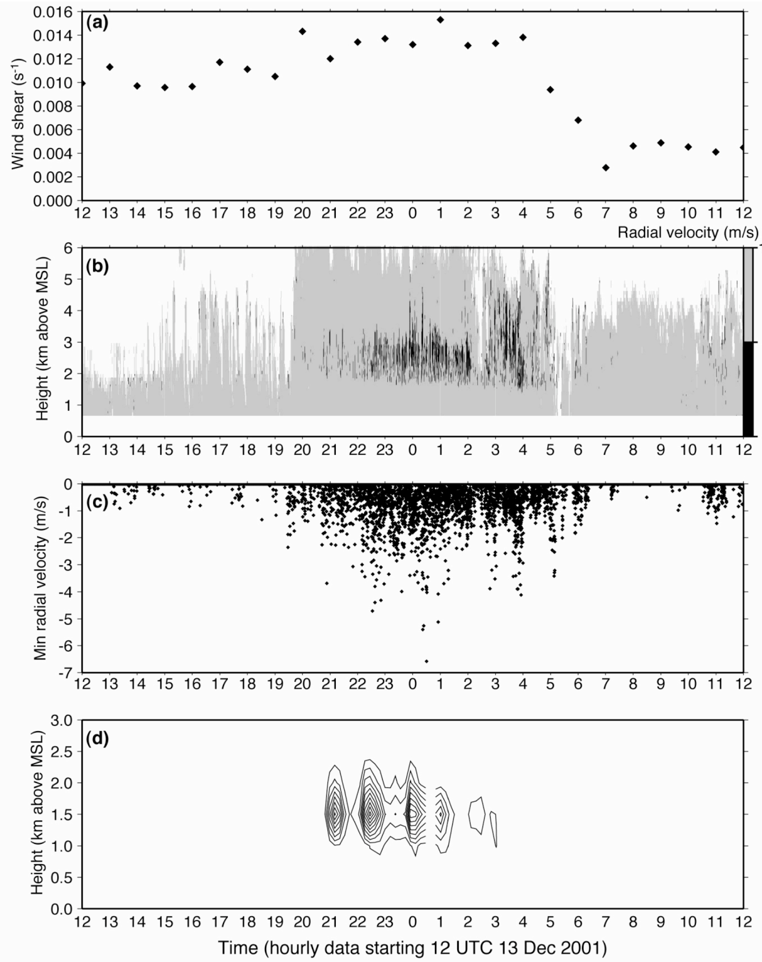

Figure 3. (a) Time series of wind shear from 0.66 to 3.0 km above MSL from a NOAA/ETL vertical wind profiler located at McKenzie Bridge, Oregon, 13-14 December 2001 during IMPROVE II. (b) Time series of radial velocity from the NOAA/ETL S-band vertically pointing radar, which was also located at McKenzie Bridge. (c) Time series of the minimum S-band radial velocity in the 2-3 km layer. (d) Time series of the frequency of occurrence of echo with low ZDR and high dBZ (dry aggregates or graupel) according to the S-Pol radar microphysical particle identification algorithm in an eastward-looking sector from 10-60 km ranges (contour interval: 0.02).

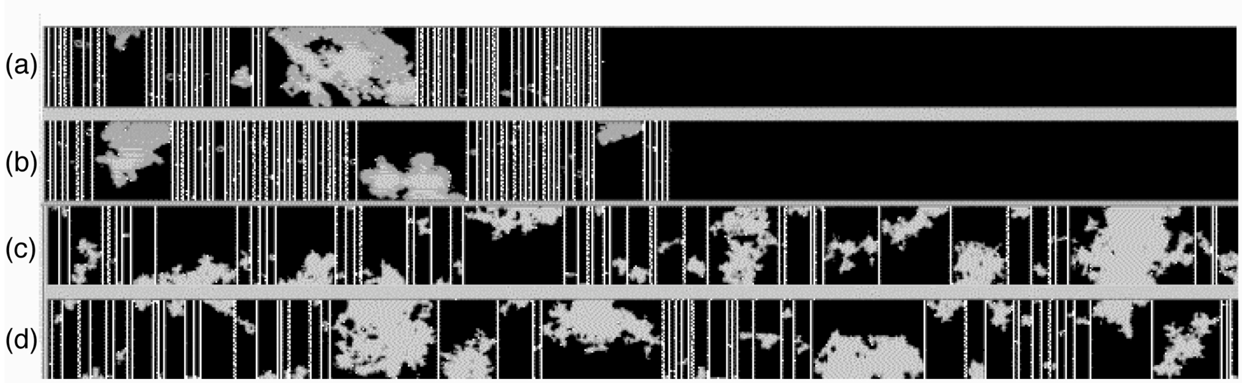

Figure 2. Ice particle imagery taken with Particle Measuring Systems probes on a NOAA WP-3D aircraft at an altitude of 2 km, ~60 km to the south of the S-Pol radar at 0126 UTC 14 December 2001 during IMPROVE II with (a)-(b) 2DC probe (width = 1.6 mm) and (c)-(d) 2DP probe (width = 9.6 mm).